FORMULATION FOR ORAL ADMINISTRATION OF LACTOFERRIN VIA ENCAPSULATION IN BOVINE SERUM ALBUMIN AND TANNIC ACID MULTILAYERS

Ece Kilic[1,2], Marina V. Novoselova[1,3], Su Hui Lim[1], Nikolay A. Pyataev[4], Sergey I. Pinaev[4], Oleg A. Kulikov[4], Olga Sindeeva[3], Oksana Mayorova[3], Murney Regan[5], Maria N. Antipina[1], Brendan Haigh[5], Gleb B. Sukhorukov[6], Maxim V. Kiryukhin*[1]

[1] Institute of Materials Research and Engineering, Agency for Science, Technology and Research (A*STAR), 2 Fusionopolis Way, Innovis, #08-03, 138634, Singapore, E-mail: kiryukhin-m@imre.a-star.edu.sg, Phone: +65 64168965

[2] Food Science and Technology Programme, Department of Chemistry, National University of Singapore, 3 Science Drive 3, 117543, Singapore

[3] N.G. Chernyshevsky Saratov State University, 83 Astrakhanskaya Street, Saratov, 410012, Russia

[4] National Research Ogarev Mordovia State University, 68 Bolshevistskaya Str., Saransk, Republic of Mordovia, 430005, Russia

[5] AgResearch Limited, Ruakura Research Centre, Bisley Road, Private Bag 3123, Hamilton 3240, New Zealand,

[6] School of Engineering and Materials Science, Queen Mary University of London, Mile End Road, London E1 4NS, United Kingdom

lactoferrin, functional foods, protection, targeted delivery, multilayer capsules, Layer-by-Layer assembly, gastric and intestinal digestion

Lactoferrin (Lf) has considerable potential as a functional ingredient in food, cosmetic and pharmaceutical applications. However, the bioavailability of Lf is limited as it is susceptible to digestive enzymes in the gastrointestinal tract and can't be delivered in native state. In order to preserve Lf the shells comprising alternative layers of bovine serum albumin (BSA) and tannic acid (TA) were tested as a system for encapsulation and oral administration of Lf. Lf absorption by freshly prepared porous 3 μm $CaCO_3$ particles followed by Layer-by-Layer assembly of the BSA-TA shells and dissolution of the cores were suggested as the most efficient and harmless Lf loading method. The Lf distribution among the microcapsules was normal with a span of 0.92. The microcapsules showed high stability in simulated gastric conditions and effectively protected encapsulated proteins from gastric digestion. Protective efficiency was found to be 76 ± 6% and 85 ± 2%, for $(BSA\text{-}TA)_4$ and $(BSA\text{-}TA)_8$ shells, respectively. Subsequently, in the simulated intestinal conditions the shells degraded releasing the Lf proteins. The Lf transit along the gastrointestinal tract (GIT) of mice was followed in vivo, and ex vivo using Bioluminescence. Lf biodistribution in different parts of the mice' GIT and in liver was examined. We have demonstrated release of encapsulated Lf in the small intestine where it is adsorbed into the bloodstream demonstrating 2-4 times higher levels compared to free Lf.

INTRODUCTION

Lactoferrin (Lf) is a whey protein that has considerable potential as a functional ingredient in food, cosmetic and pharmaceutical applications. Lf possesses various biological functions such as antibacterial, antiviral, antitumor, antifungal, anti-inflammatory, immunomodulatory, analgesic, antioxidant, enhancement of lipid metabolism, etc. [1-6]. In addition, it is low-cost and displays no toxic side effects. The major challenge that hinders its wide application is its poor in vivo stability due to rapid degradation by proteolytic enzymes. When intravenously injected, the plasma half-life of Lf is several minutes and frequent administration is necessary to achieve a therapeutic effect [2]. Oral administration is natural and non-invasive way for supplementing Lf, since important receptors of Lf in the body are the intestinal mucosa and gut-associated lymphatic tissue (GALT)- related cells [3, 7-10]. Newborn infants and mammals enjoy the full benefits of Lf with milk consumption that is essential for their development. As they grow up, the maturation of the digestive system with age results in complete Lf digestion [1]. Lf breaks down into several large fragments by the gastric digestive enzyme, pepsin, but in case of direct intra-duodenal administration it may reach intestine and exist there for a few hours [3]. Another barrier for Lf bioavailability is its poor permeability across the intestinal epithelium because of the high molecular weight and lack of lipophilicity [2, 4]. However, only the intact native Lf may reach the GALT and enter the lymphatic system, which is the site of its most beneficial action.

In this regard, there is a high demand for an appropriate Lf delivery system that should protect Lf from digestion in stomach and facilitate its permeability across intestinal epithelium. During the past decade, several oral Lf delivery systems have been suggested [2-8, 11-15]. Nojima et al. first synthesized Lf conjugated with branched 20 kDa poly(ethylene glycol) (PEG) which

demonstrated a significantly higher resistance to pepsin proteolysis in the mature rats [13]. The proteolytic half-life of the PEGylated Lf was found to be two times longer and its absorption from the rat intestinal tract increased ten times compared to unmodified Lf. Liposomes have also been used for Lf encapsulation [7, 10-12, 15]. Yamano et al. demonstrated that Lf encapsulated in liposomes had better resistance to digestive enzymes, thus enhancing the inhibitory effect of orally administered Lf on alveolar bone resorption using lipopolysaccharide-induced periodontitis rat models [10]. Onishi et al. developed a chitosan/alginate/Ca- microparticles, which were sufficiently small to enter the mucous layer of intestine [5]. Lf encapsulated in those microparticles showed better anti-inflammatory properties compared to free lactoferrin in a rat model with induced edema. However, the major drawbacks of all these systems are the use of organic solvents and harsh encapsulation conditions that may result in a significant loss of Lf bioactivities.

At present, method of Layer-by-Layer (LbL)-assembly to make multilayer microcapsules has been widely used for various applications as it is highly versatile with respect to payload and offers various targeted delivery and triggered release options, such as light, magnetic field, ultrasound, temperature, pH, salinity, redox potential, and others [16-21]. This technology is specifically advantageous for encapsulation of fragile cargo in biomedical and functional foods applications, as it may utilize only aqueous solutions and be performed at room temperature. Enzymatic cleavage is the release mechanism particularly important for these applications. Enzymatically degradable microcapsules have been extensively investigated during the last decade [22-31] and employed for delivery of genes [22, 24], growth factors [27, 28] and vaccines [29-31]. The main drawback of all these microcapsules was the use of expensive and significantly cytotoxic polycations. Recently, we reported LbL-assembled multilayer

microcapsules made of low-cost and food grade ingredients (tannic acid (TA) and bovine serum albumin (BSA)) exploiting the ability of tannins to precipitate proteins by hydrogen bonding and hydrophobic interactions [32, 33]. The microcapsules demonstrate low cytotoxicity, they are resistant towards treatment with trypsin but susceptible to α-chymotrypsin, the two proteolytic enzymes with different cleavage site specificity [33]. Incorporation of TA into the shell has an additional benefit providing the microcapsules with anti-oxidant properties by scavenging Fe2+ ions [34].

In this work for the first time we introduce the LbL-assembled BSA-TA microcapsules as a system for encapsulation and oral delivery of a bioactive ingredient, Lf. We demonstrate the efficiency of Lf loading into the microcapsules, their behavior under simulated gastrointestinal conditions and the efficiency of proteins protection in gastric environment. Finally, we follow the transit of Lf-containing capsules along the gastrointestinal tract (GIT) of mice in vivo, and ex vivo Lf biodistribution in different parts of the mouse GIT and in liver using Bioluminescence.

MATERIALS AND METHODS

Materials. The bioactive Lf from bovine whey was kindly supplied by the Tatua Cooperative Dairy Company Ltd (New Zealand). Poly-L-Lysine hydrochloride (PLL, Mw 15,000 – 30,000), BSA lyophilized powder (≥96%), TA (ACS grade), BSA conjugated with tetramethylrhodamine isothiocyanate (BSA/TRITC), bile salts (for microbiology), pancreatin from porcine pancreas (≥ 100 USP U/mg), pepsin from porcine gastric mucosa (3802 U/mg), mini protease inhibitor cocktail cOmplete™, hydrochloric acid, calcium chloride dehydrate, sodium bicarbonate (for molecular biology), sodium chloride, sodium hydroxide, acetonitrile (for HPLC, ≥99.9%) were purchased from Sigma-Aldrich. Anhydrous sodium carbonate (ACS, 99.5% min) was purchased

from Alfa Aesar. 0.1% aqueous solution of trifluoroacetic acid (TFA, LC/MS grade, ≥99.99%) was purchased from VWR Chemicals. DQ™ Red BSA was purchased from Molecular Probes Inc, USA. The bovine lactoferrin ELISA kit was purchased from Bethyl Laboratories, Inc., USA. Cyanine 7 N-hydroxysuccinimide ester (Cy7-NHS) was purchased from Lumiprobe Corporation, USA. Cy7-labelled Lf (Cy7-Lf) has been prepared according to a standard protocol provided by Lumiprobe Co and purified by dialysis. All chemicals were used as received without further purification. Deionized (DI) water (specific resistivity higher than 18.2 MΩcm) from Milli-Q plus 185 (Millipore) water purification system was used to make all solutions.

Preparation of Lf-loaded microcapsules. BSA-TA capsules loaded with proteins (Lf, Cy7-Lf, BSA-TRITC or DQ™ Red BSA) were prepared with assistance of a $CaCO_3$ sacrificial template, as depicted in Figure 1. Spherical porous $CaCO_3$ particles with an average diameter of ~3 μm (corresponding SEM images are available in the Supporting information) were synthesized according to Volodkin et al. [35]. In post-loading, 0.6 mL of 1M $CaCl_2$ and Na_2CO_3 solutions were injected into 1.8 mL of DI water under vigorous agitation. 2 min later agitation was stopped and $CaCO_3$ particles were separated by centrifugation and washed two times with DI water. Subsequently, the particles were re-dispersed in 30 mg/mL Lf aqueous solution and shaken for 15 min, followed by centrifugation and two washing steps to remove unabsorbed proteins. In co-precipitation, 1.8 mL of an aqueous protein solution (30 mg/mL Lf or 1 mg/mL DQ™ Red BSA) was mixed with 1M $CaCl_2$ solution (0.6-0.8 mL) followed by injection of 1M Na_2CO_3 (0.4-0.6 mL) under vigorous agitation, followed by centrifugation and two times washing by DI water.

LbL assembly of BSA-TA shells was performed as the following. First, $CaCO_3$ microparticles with absorbed proteins were immersed in 5 ml of 2 mg/mL PLL solution in order to generate the first anchoring layer and ensure integrity of the capsules [33]. After 15 min of continuous shaking, the microparticles were collected by centrifugation and residual PLL was removed by washing them twice with DI water. Further alternating layers of BSA and TA were introduced, each from 5 mL of 2 mg/mL solution with two washing steps after each layer. This procedure was repeated to achieve desired number of BSA-TA bilayers. Finally, the particles were redispersed in DI water and $CaCO_3$ was dissolved by adding 1M HCl solution dropwise until pH reaches ~3.0. The resulted capsules were collected by centrifugation and washed two times with DI water.

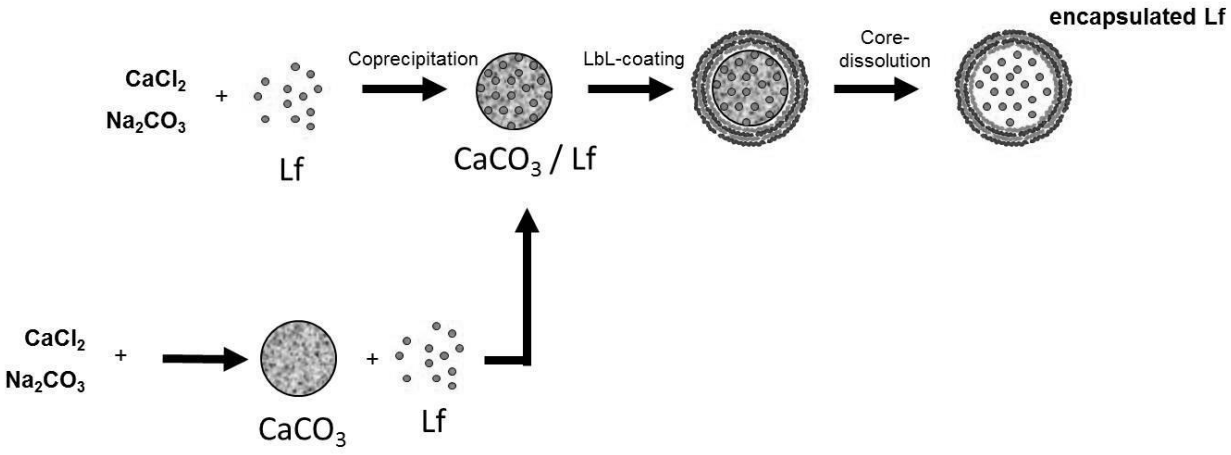

Figure 1. Scheme of Lactoferrin (Lf) encapsulation: co-precipitation of $CaCO_3$ and Lf vs adsorption of Lf in porous $CaCO_3$ microparticles followed by Layer-by-Layer deposition of bovine serum albumin and tannic acid and final dissolution of $CaCO_3$.

***In vitro* digestion method.** Capsules behavior under simulated gastrointestinal conditions has been studied at 37 °C under continuous agitation using the following protocol [36]. 4 mL of 150 mM NaCl solution at pH 3 (acidified by HCl) was added to 5 mL of a suspension containing ~

1mg of encapsulated protein. Then 1 mL of 7.1 mg/mL pepsin solution containing 150 mM of NaCl at pH 7.0 was injected there (pepsin final concentration was 180 Units per 1 mg of a protein). This was considered as a starting point for digestion. At 60 min of digestion, pH of the solution was increased to 7.0, then 1 mL of 120 mM bile salts (containing 0.1 M $NaHCO_3$ solution at pH 7.0) and 1.0 ml of 18 mg/mL pancreatin solution (pancreatin final concentration was 12 USP U/mg protein) were added. To stop digestion at a selected point of time, pH of the solution was increased to 7.0 (with a predetermined amount of NaOH), a protease inhibitor tablet was added and the solution was frozen at -20^{o}C before further analysis. For weight loss experiments, all the samples were defrozen, the capsules were separated by centrifugation, washed two times with DI water and freeze-dried for 2 days using Console Freeze Dry System from Labconco.

***In vivo* digestion and *ex vivo* Lf biodistribution studies.** A total of sixteen BALB/c female mice were used in this study. Animal ethics clearance was approved by the ethical committee of National Research Ogarev Mordovia State University, Russia. The abdomen of each animal was carefully shaved to improve fluorescence acquisition. 0.3 mL of a suspension containing 4 mg of encapsulated Cy7-Lf was dosed directly into the stomach of eight mice *via* oral gavage. A control group of eight mice was dosed with solutions of free Cy7-Lf. Prior to imaging, animals were anaesthetized by intramuscular injection of zoletil (50 mg/kg) and placed in an imaging cradle. The mice were imaged at 0.05, 0.5, 1, 5, 8 and 24 h after dosing with an IVIS imaging system (Xenogen Corp.) using excitation/emission at 675/810-875 nm. Photons were quantified using LivingImage software (Xenogen Corp). To improve fluorescence quantitation, two mice from each group have being euthanased by cervical dislocation for further *ex vivo* analysis at each time point in the range from 1 to 24 h. For all animals, the gastrointestinal tracts and liver

were removed and imaged. At 0.05 and 0.5 h post-administration, Lf was mostly located within the stomach and other organs demonstrate autofluorescence only. Therefore, in order to save the animals, levels of fluorescence in stomach and proximal parts of small intestine were estimated from *in vivo* measurements using the corresponding damping coefficients determined for mice sacrificed at later time points.

Characterization. Concentration of released Lf in aqueous solutions was independently measured by bovine lactoferrin ELISA kit (Bethyl Laboratories, Inc., USA) following their standard protocol and by high performance liquid chromatography (HPLC) using a Waters 2695 Alliance System equipped with 2996 photo diode array detector. The column was Phenomenex Aeris XB-C8, particle diameter 3.6μm WIDEPORE, 4.6 mm x 100 mm. Prior to analysis, all the samples were filtered through a 0.45 μm syringe filter, the injection volume of sample was 50 μL and detection wavelength was at 210 nm. A continuous gradient elution at 35 ^{o}C and 1.0 ml/min flow rate was performed with 0.1% aqueous TFA solution (mobile phase A) and 90% acetonitrile – 10% aqueous TFA solution (mobile phase B) as following: the percentage of the mobile phase B was increased linearly from 20 to 50% by 15 min, then decreased back to 20% by 20 min of elution. All of the experiments were done in triplicate.

Quantification of lactoferrin incorporated into capsules was performed by western blot. Capsules were re-suspended in 8M Urea, 50mM Tris pH 8.9 and incubated for 1 h. Protein concentration was determined using the Bradford method [37] and 1 μg, 0.4 μg, 0.2 μg and 0.1 μg of protein was separated on 10% BisTris NUPAGE gels (Life Technologies) with a dilution series of purified Lf (2.5 μg to 0.025 μg). The protein was transferred onto nitrocellulose membranes (Pall Corporation, East Hills, NY, USA). Membranes were blocked in Tris-buffered saline (TBS) solution (0.05 M Tris-HCl, 0.15 M NaCl, pH 7.6) containing 0.1% Tween 20

(TBST) and 5% BSA for 2 h. After three washes in TBST containing 0.1% BSA, membranes were incubated for 2 h in TBST containing 0.1% BSA with 1:60000 dilution of anti-Lf antibody (JWT88b, rabbit polyclonal antibody raised against purified bovine Lf). Following three further washes in TBST containing 0.1% BSA, membranes were incubated for 1 h in TBST containing 0.1% BSA with a 1:10000 dilution of goat anti rabbit secondary antibody conjugated to horseradish peroxidase (Sigma-Aldrich Co Ltd, Gillingham, United Kingdom). Finally membranes were washed in TBST containing 0.1% BSA three times and then washed a further four times in TBS. To visualize the immunoreactive bands, membranes were incubated for 1 min in ECL Western blotting detection reagents (Amersham, GE Healthcare, Buckinghamshire, United Kingdom) and then detected using the ImageQuant LAS 4000 imaging system (GE Healthcare Biosciences, Pittsburgh, PA, USA). The densities of immunoreactive bands were determined using Quantity One software (BioRad, Hercules, CA, USA).

Scanning electron microscopy (SEM) analysis was performed using field-emission scanning electron microscope (FE SEM JSM-6700F). Samples were prepared by depositing a drop of particles or capsules suspension on a silicon wafer allowed to dry at room temperature. Before imaging, the samples were coated with approximately 20 nm gold film using a Denton sputter-coater.

Time-of-flight secondary ions mass spectroscopy (ToF-SIMS) analysis was conducted using ToF-SIMS-IV instrument (ION-TOF GmbH, Germany). Positive secondary ions were detected, since Fe^+ has a high yield of positive ions. For the measurement, a suspension of capsules was deposited on a copper substrate, dried in hot air (50-60 ^oC) and put under vacuum. The copper was used here because the ion yield from a pure Cu surface is very low. To remove any surface contamination from air and evaporated solution, a second beam of 1 keV Ar^+ with 12 nA current

scanned over a 200 μm x 200 μm area was used. Disappearance of the organic secondary ions from the Cu surface upon sputtering, was chosen as a criterion for complete removal of the surface contamination. At the same time, such sputtering also removed the shell of the capsules and allowed analysis of their internal content. Then the analysis beam of 25 keV Bi^+ with 1 pA average current was rastered over a 50 μm x 50 μm area and a mass spectrum was obtained from each pixel of this scan. Focusing of the analysis beam provided a lateral resolution better than 1 μm. The peaks corresponding to C and Fe positive ions were identified in the mass spectra, their intensities were integrated and plotted versus primary ion beam position. Thus, mass resolved images were obtained.

The measurements of fluorescence intensity have been performed using PerkinElmer Luminescence Spectrometer LS 55. The emission spectra have been recorded over a range of 595 - 720 nm wavelengths; excitation wavelength was 590 nm, the emission slit widths was 10 nm, and the scanning speed was 50 nm/min. All measurements have been performed using disposable polystyrene cuvettes with optical path length of 10 mm at room temperature (22 ^oC). All the emission spectra registered had maximal intensity at 620 nm.

RESULTS AND DISCUSSION

Lactoferrin encapsulation efficiency. In this work, encapsulation of Lactoferrin was performed through its absorption by porous $CaCO_3$ microparticles, as first suggested by Volodkin et al. [35]. This material has a number of advantages including easy synthesis and cheap precursors, it is non-toxic and approved for the use as additive in foods by FDA, Food Safety Commission in Japan, and in many other countries. Here we have tried two different approaches to load $CaCO_3$ with Lf, as depicted in Figure 1. In the first approach, formation of

microparticles occurred in the presence of protein macromolecules (30 mg/mL Lf solution), while in the second approach $CaCO_3$ particles were first formed and washed and then put in contact with Lf aqueous solution of the same concentration. To measure the amount of absorbed Lf, the particles were washed two time in DI water and then dissolved in 1M HCl. Concentration of released Lf was measured by ELISA and HPLC. Table 1 shows the results of these measurements (calibration curve and respective chromatograms are available in Supporting Information).

Table 1. Amount of lactoferrin absorbed by $CaCO_3$ particles.

Approach	Weight of $CaCO_3$ microparticles, mg	Amount of released Lactoferrin, mg	Lactoferrin absorbed, wt%
Co-precipitation (pH >10)	60	0.3 [a]	0.5
Co-precipitation (pH 8)	48	1.0 [a], 1.2±0.3 [b]	2.5±0.6
Post-loading	60	0.7±0.1 [b]	1.2±0.2
	300	4.1±1.5 [b]	1.4±0.5
	600	7.6 [b]	1.3

Methods to measure Lf concentration: [a] - ELISA; [b] – HPLC.

The lowest amount of released Lf was achieved from samples prepared *via* the co-precipitation approach, when stoichiometric amounts (6×10^{-4} moles) of $CaCl_2$ and Na_2CO_3 were mixed in the presence of Lf macromolecules. This low amount of released Lf might be due to high pH value in the resulted dispersion (pH > 10) caused by the injection of highly alkaline sodium carbonate solution as Lf treatment with 1M sodium carbonate resulted in complete degradation of the protein (see Supporting information). In order to reduce the degradation of Lf, pH of the reaction mixture was decreased from >10.0 to 8.0 by increasing the ratio of $CaCl_2$ concentration to that of Na_2CO_3 from 1.0:1.0 to 1.5:1.0. In these conditions, four times more intact Lf was released from

$CaCO_3$ particles. However, the chromatograms of respected samples demonstrate that the peak at retention time of 9.5 min (corresponding to native Lf, see Figure 2, line 1) becomes broader and several more intense peaks appear at the lower retention times (see Figure 2, line 2). The possible reason could be partial breakdown of Lf during co-precipitation into smaller fragments. To overcome this problem, post-loading approach was suggested where $CaCO_3$ particles were formed first and washed two times with DI water to remove all salts and neutralize the pH. These particles were later introduced to a solution of Lf. The chromatogram of released proteins (Figure 2, line 3) demonstrates narrow peak at 9.5 min as in native Lf and another narrow peak of comparable intensity at lower retention time of 8.3 min. Thus Lf still breaks down during absorption by the particles at post loading, however, degradation is significantly lower than in co-precipitation approach. Taking into consideration the need to encapsulate higher amount of native Lf, post-loading approach was chosen for further experiments.

Linear growth of the amount of encapsulated Lf was found when 5 and 10 times more $CaCO_3$ particles were introduced into the Lf solution providing nearly constant ~ 1.2-1.4 wt. % of encapsulated Lf (see Table 1). This means that the chosen concentration of Lf solution (30 mg/mL) was adequate to ensure saturation of all microparticles with Lf to their maximum capacity.

In the next step, LbL assembly of the BSA-TA shells was performed on the surface of $CaCO_3$/Lf particles followed by dissolution of the core material with HCl. Figure 3-a shows SEM image of thus formed capsules. As the magnified image of insert shows, they have rough surface and shape close to spherical.

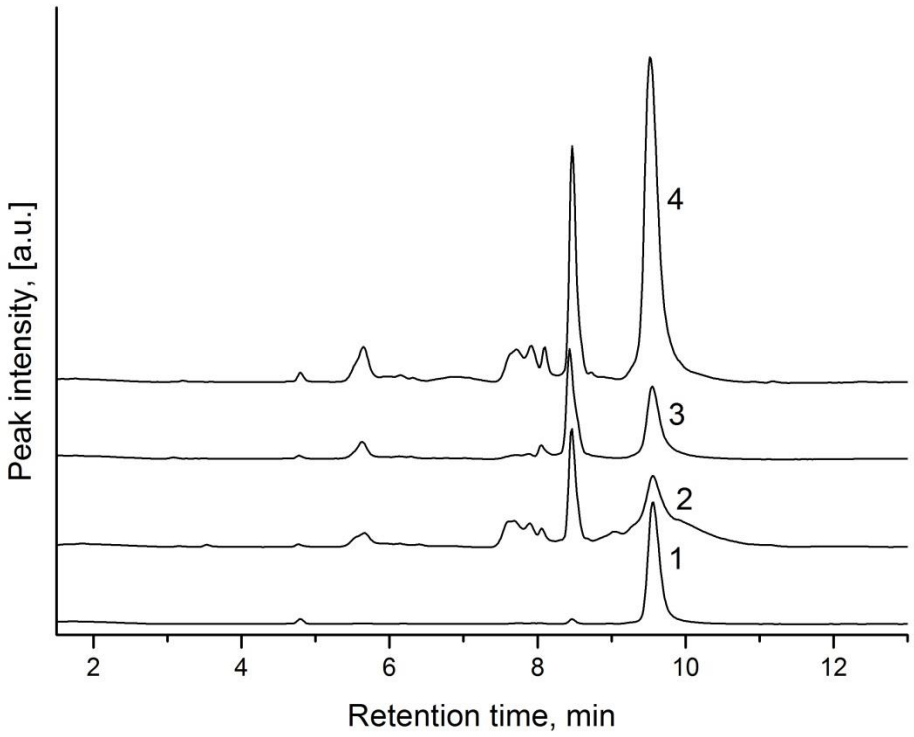

Figure 2. HPLC chromatograms of (1) a standard 1 mg Lf solution in DI water, and Lf released from $CaCO_3$ microparticles upon their dissolution at pH 3. Lf was (2) co-precipitated with 48 mg $CaCO_3$ at pH 8; (3) post-loaded to 60 and (4) 300 mg of $CaCO_3$. Volume of all samples was 6 mL.

In order to measure the amount of Lf in the final capsules, they were treated with 8M urea solution. Under these conditions all the capsules were disintegrated and all the proteins (BSA, LF) underwent denaturation. The resulted solution has been tested by western blot (see Supporting information, SI Figure 6). The capsules fabricated from 300 mg $CaCO_3$ microparticles by the post-loading approach contained 0.72 mg of encapsulated Lf and 6 mg of total proteins (including BSA and Lf, both intact and fragmented). If compared to 4.1 mg of Lf absorbed in $CaCO_3$ microparticles (see Table 1), one can see that only ~ 18% of initially

encapsulated Lf retained inside upon LbL assembly and dissolution of the core and the rest was lost.

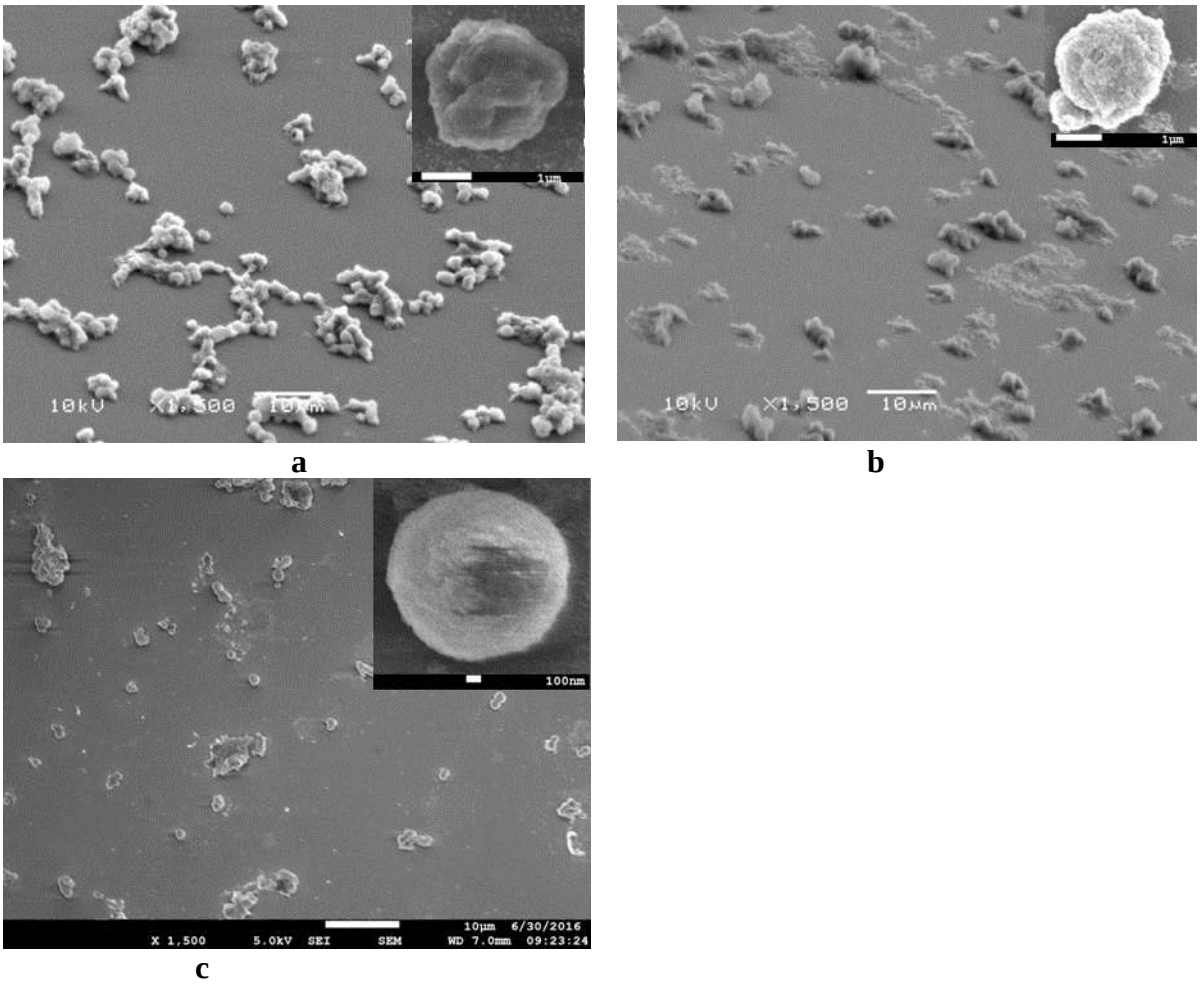

Figure 3. SEM images of Lf/(BSA-TA)$_4$ capsules after (a) core dissolution, (b) 60 min of treatment in simulated gastric fluid and (c) 3 min of treatment in simulated intestine fluid.

Interesting that there was higher amount of released Lf in the sample obtained by co-precipitation approach from 240g $CaCO_3$ (0.9 mg of Lf and 4.5 mg of total proteins). The possible reason is that in the former case proteins can be absorbed only by the pores "opened" onto the particles surface and diffusion of Lf macromolecules deep inside narrow pores of

$CaCO_3$ microparticles could be hindered. In the latter case occlusion of proteins into the cavities "closing" upon further growth of the particles may occur. As a result, co-precipitation approach allows absorption of more Lf, both intact and damaged fragments.

HPLC and western blot show the total amount of encapsulated Lf in a batch but provide no information about its amount in an individual microcapsule and the distribution of Lf among the microcapsules in the batch. Lf has a high affinity to Fe^{3+} and is believed to play a major iron-regulating role in new born infants and mammals [1]. Since Fe gives high ionization yield and ToF-SIMS provides submicron spatial resolution, it allows detection of the amount of iron-containing protein in individual capsules [38]. Fig. 4-a shows the C^+ and Fe^+ distribution maps for a sample of Lf-loaded BSA-TA microcapsules. It can be seen that the image of Fe^+ correlates with that of C^+. Since these ions originate from the protein, the bright spots show the location of capsules on the copper substrate. To quantify the amount of the encapsulated Lf, the ratio of Fe and C peak intensities was calculated for each individual measured capsule. Note that this ratio is the ratio of ion intensities, which depends on ionization yield of the elements. The ionization yield of Fe is several orders of magnitude higher than that of C. After dozens of capsules of each type were evaluated, the distribution of this ratio over the capsules in a batch was plotted (see Figure 4-b). The distribution can be well fitted with a Gauss curve, where the mean Fe/C ratio (R) was found to be 0.54 ± 0.16, and the polydispersity index or span defined as (R90 – R10)/R50 = 0.92.

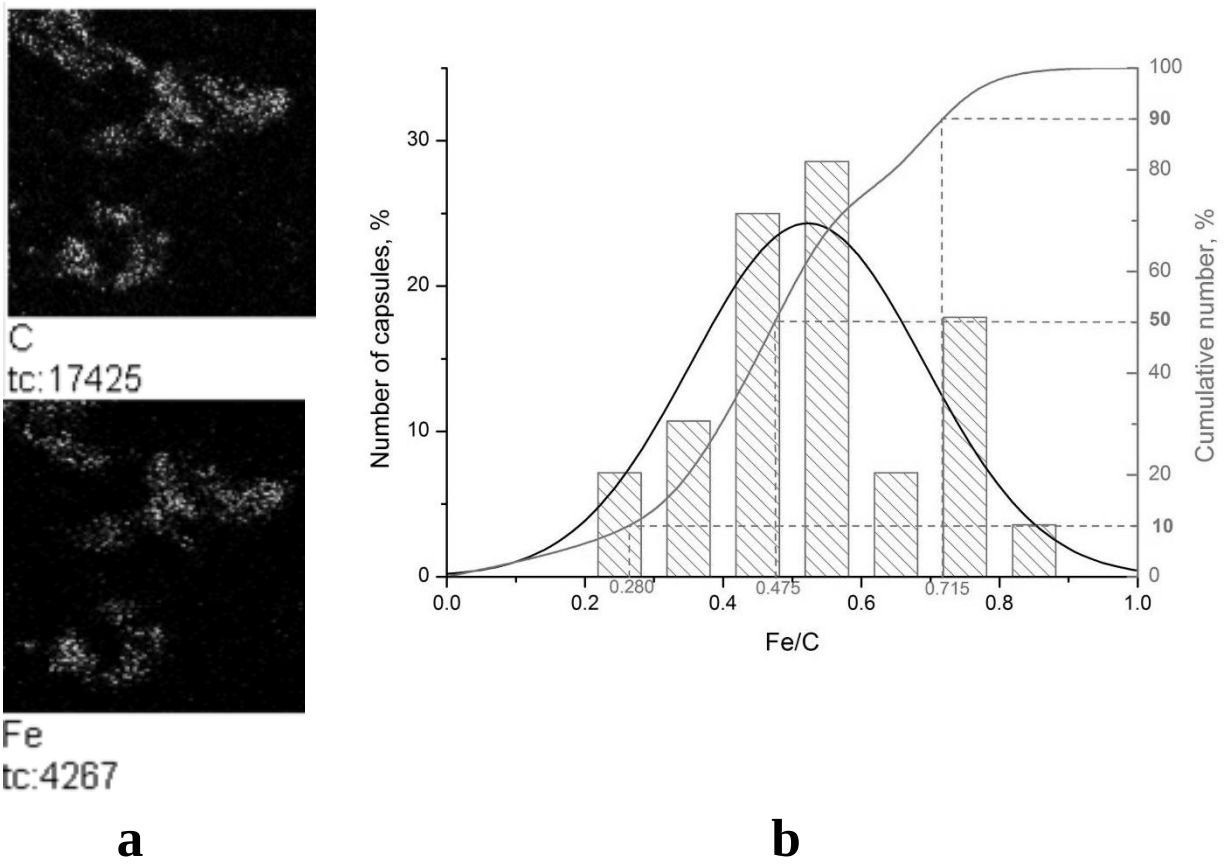

Figure 4. (a) Mass resolved images (chemical maps) of positive ions from Lf-loaded capsules, scan size 50 μm x 50 μm; (b) histogram of Fe/C ratio showing distribution of Lf among individual capsules.

***In vitro* digestion study of encapsulated Lf.** The performance of encapsulated Lf in gastrointestinal tract was evaluated using *in vitro* simulated digestive model [36]. Table 2 shows the weight of empty and Lf-loaded $(BSA\text{-}TA)_4$ capsules, as prepared and upon simulated digestion.

Table 2. Weight and corresponding weight loss of Lf/$(BSA\text{-}TA)_4$ capsules upon their treatment with simulated gastric (SGF) and intestine (SIF) fluids.

	Weight, mg	Weight loss, %
$CaCO_3$ / $(BSA\text{-}TA)_4$	317.2 ± 6	-
$(BSA\text{-}TA)_4$	15 ± 2	-
$Lf/(BSA\text{-}TA)_4$	32.1 ± 3	0
SGF, 60 min	30.6 ± 1	5
SIF, 3 min	9 ± 2	72
SIF, 10 min	1.10 ± 0.08	96.6
SIF, 60 min	0.9 ± 0.6	97.2

As table 2 shows, treatment with HCl at pH 3 dissolves all $CaCO_3$ (~300 mg) from the capsules' cores. The capsules loaded with Lf are nearly two times heavier than empty capsules that may be an indication of the amount of both intact Lf and its fragments in the capsules. However, the possible effect of Lf absorbed by $CaCO_3$ particles on the later process of BSA-TA shell assembly on their surface making it thicker and/or denser will not be excluded. The corresponding SEM images show that the Lf-loaded capsules look as spheres while the capsules without Lf are partially collapsed (see Figure 3-a and SI Figure 3). If one compares the weight of $Lf/(BSA\text{-}TA)_4$ capsules (32.1 mg) with the total protein weight (6 mg, BSA + Lf) detected by western blot after capsules were completely degraded in 8M urea (see above), then the major component of the capsules is TA.

The Lf-loaded capsules remain stable and do not degrade in the SGF, the observed weight loss after 60 min of treatment is within experimental error. SEM analysis also does not show significant changes in the capsules size or shell integrity (see Figure 3-b). However, fast degradation of the capsules occurs in SIF demonstrating the loss of ~70 % of initial weight after 3 min and nearly complete degradation after 10 min of SIF treatment. SEM image of capsules

treated in SIF for 3 min demonstrate less number of capsules as shown in Figure 3-c. A cave on the shell's surface clearly seen in the insert to this figure may be an indication of the very beginning stage of capsules' degradation.

The reason for such drastic changes in shells' stability could be different cleavage site specificity of pepsin and pancreatin. Pancreatin cleaves peptide chains mainly at the carboxyl side of the amino acids lysine or arginine and their total amount in BSA is rather high (18.72% [39]). Contrary, pepsin preferentially cleaves peptide amide bonds when large hydrophobic amino acid (tyrosine, tryptophan, or phenylalanine) are at the carboxyl side and BSA contains only 6.56% of phenylalanine, 5.06% of tyrosine, and 0.58% of tryptophan [39].

In order to study the protection of proteins against gastric digestion using LbL-assembled shells, DQ™ Red BSA protein was used for encapsulation instead of Lf. This protein is heavily labeled with BODIPY dyes and, when in intact native confirmation, it doesn't show fluorescence due to strong quenching effect. This quenching is relieved upon protein hydrolysis to smaller dye-labeled peptides by proteases. In order to match concentration of DQ™ Red BSA in the samples, the sample with free unprotected protein was prepared as the following. First DQ™ Red BSA was loaded into $CaCO_3$ microparticles by the same post-loading approach as for microcapsules preparation, then the particles were dissolved by acidifying the solution to pH 3 with HCl and the resulted solution was exposed to SGF. The fluorescent intensity was increased during 60 min due to gradual digestion of the protein, as shown in Figure 5 (line 1). Contrary, the samples with DQ™ Red BSA encapsulated in $(BSA\text{-}TA)_4$ and $(BSA\text{-}TA)_8$ shells demonstrated some increase in fluorescent intensity within first 10 min of digestion only, hardly any changes in the fluorescence were observed upon further digestion from 10 to 60 min (Figure 5, lines 2, 3). Moreover, its intensity level was significantly lower than in the sample with free unprotected

DQ™ Red BSA. In order to quantify this effect, we introduce a protective efficiency parameter, P.E., which is defined as following:

$$P.E. = (1 - I_x/I_0) \times 100\%,$$

where I_x is a fluorescence intensity of DQ™ Red BSA encapsulated in $(BSA\text{-}TA)_4$ or $(BSA\text{-}TA)_8$ shells, and I_0 is the fluorescence intensity of unprotected protein at the same point of digestion time. After 60 min of treatment, P.E. was found to be 76 ± 6% and 85 ± 2% for $(BSA\text{-}TA)_4$ and $(BSA\text{-}TA)_8$, correspondingly. This observation of initial increase in fluorescence intensity within the first 10 min of digestion could be a result of some defect loose shells within a batch that allow pepsin to penetrate inside. While the number of layers increases the defects are lesser and the amount of such loose shells decreases providing better protection.

In the *in-vitro* digestive model used in this work, intestinal digestion starts after 60 min of gastric digestion. The insert in Figure 5 shows corresponding changes in fluorescent intensity. As it was discussed above, BSA is much more susceptible to pancreatin than to pepsin digestion, so significantly higher fluorescent levels in SIF are expected. In the sample with free unprotected DQ™ Red BSA fluorescence increases dramatically from 60 to 70 min of digestion (within first 10 min of SIF treatment) and then reaches the plateau indicating complete digestion of introduced DQ™ Red BSA by this point of time. As it was shown in Table 2, BSA-TA shells degrade nearly completely within 10 min in the SIF. However digestion of encapsulated DQ™ Red BSA is delayed significantly, the fluorescence intensity increases gradually from 60 to 120 min of digestion. The reason could be some pancreatin aging as it is involved in additional degradation cycles of both the shell and encapsulated protein. Nevertheless, the fluorescence intensity of DQ™ Red BSA encapsulated in $(BSA\text{-}TA)_4$ and $(BSA\text{-}TA)_8$ shells by the end of 120 min of digestion was lower by just 10 and 25 %, respectively, when compared to unprotected

protein. This demonstrates nearly complete release of encapsulated proteins from the microcapsules as they reach an intestine.

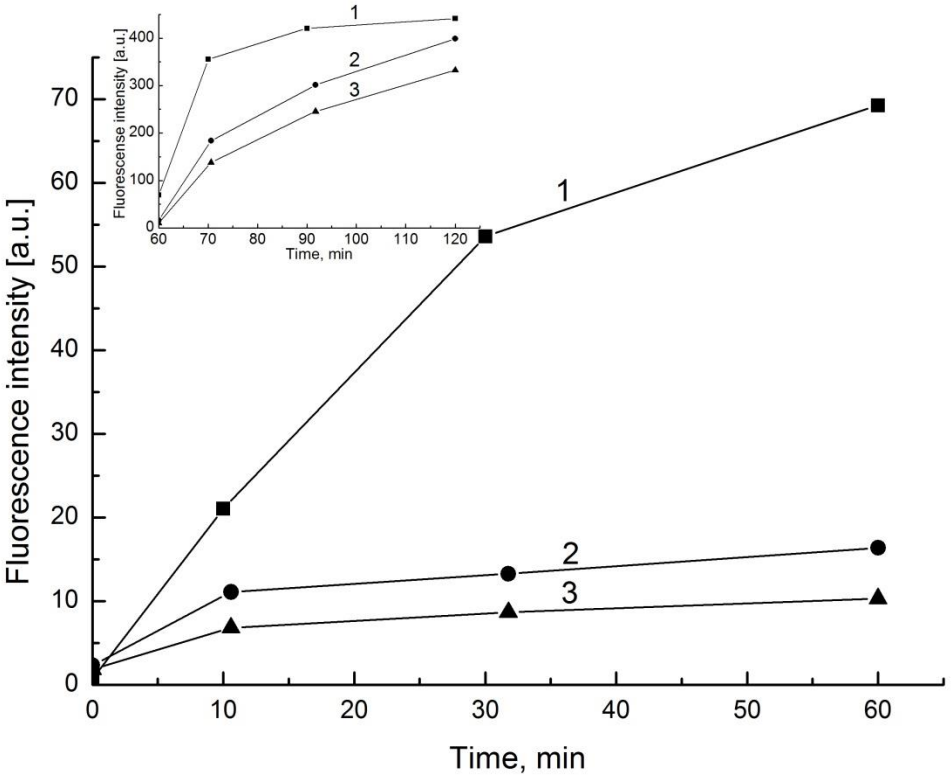

Figure 5. Fluorescence intensities with respect to digestion time in SGF of (1) free DQ™ Red BSA solution obtained upon post-loading the $CaCO_3$ microparticles with protein followed by their dissolution at pH 3; Lf encapsulated with (2) $(BSA\text{-}TA)_4$ shells and (3) $(BSA\text{-}TA)_8$ shells. The insert shows the corresponding changes with respect to digestion time in SIF.

In order to track progression of encapsulated Lf along GIT *in vivo* we have used Cy7-Lf which emits fluorescence in the near infrared region (λ_{em} = 800 nm). For small animals, the ratio of this signal to noise is high enough that allows direct and non-invasive tracking of capsules in live animals providing qualitative information on their distribution with time [40]. Figure 6 shows

progression of the dye for mice dosed with Cy7-Lf and encapsulated Cy7-Lf (Cy7-Lf_{encaps}). Again, in order to match concentration of Cy7-Lf_{encaps}, the sample with free unprotected protein was prepared by Cy7-Lf post-loading into 300 mg of freshly prepared $CaCO_3$ microparticles followed by their dissolution with HCl till pH 3. As it was shown above, ~ 4mg of Lf are absorbed in these conditions (see Table 1).

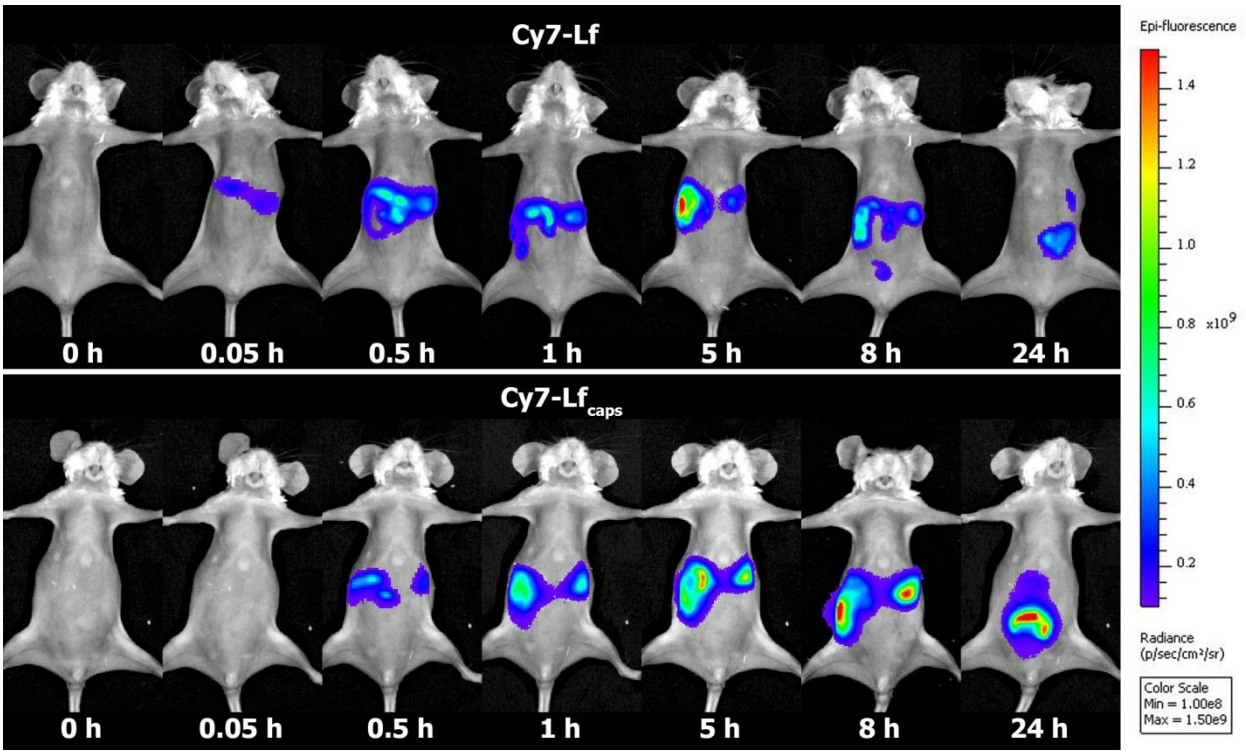

Figure 6. Mouse whole body images and corresponding Cy7 signal at 0.05, 0.5, 1, 5, 8 and 24 h after dosing with Cy7-Lf, and Cy7-Lf_{caps}.

At 0.05 h after administration, fluorescence has been detected in stomach of mice dosed with Cy7-Lf, while it was comparable to background in those dosed with Cy7-Lf_{encaps}. At 1 h, fluorescence was registered in both stomach and the proximal part of the small intestine, and at 8 h, the chymus reached large intestine for both groups. At this time point, the mice dosed with Cy7-Lf_{encaps} had very high fluorescence in the distal parts of small intestine. One possible reason could be that this part of the mouse GIT is localized closer to skin so that the optical signal is less

damped. However the mice dosed with Cy7-Lf had much lower fluorescence there. At 24 h, fluorescence was registered in the distal parts of small and in the large intestine for both groups, although for mice dosed with Cy7-Lf_{encaps} it was significantly higher.

Figure 7 shows fluorescence intensities in mouse stomach, small intestine, caecum / appendix and colon for both groups of mice. In the time span from 0.05 to 1 h, fluorescence was registered in stomach and small intestine only. At 0.05 h, it was much lower for the group of mice dosed with Cy7-Lf_{caps}, but from 0.5 h onwards this group had much higher fluorescence intensity, especially in the small intestine. For example, at 5 h time point it was 6.5 times higher than in the control group. From 5 h onwards, fluorescence was registered at caecum/appendix and colon.

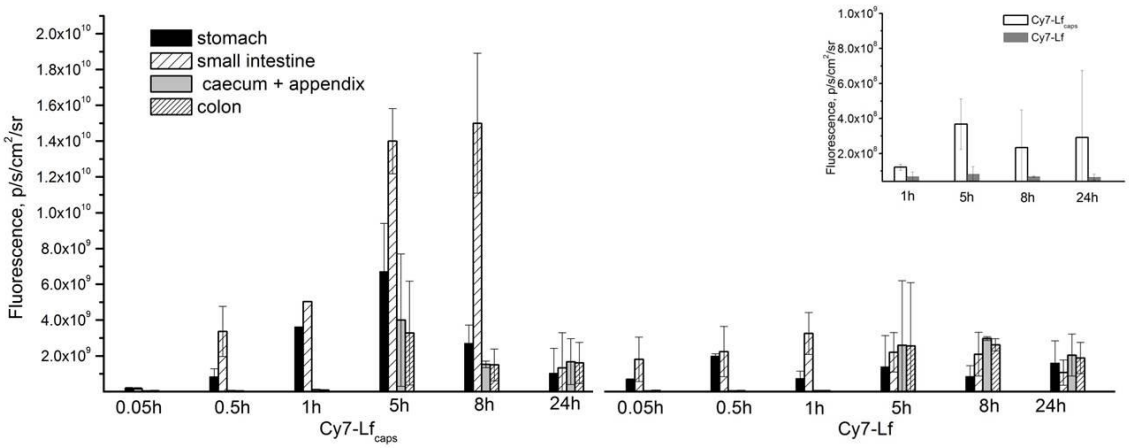

Figure 7. Fluorescence intensity in mouse stomach, small intestine, caecum/appendix, and colon at 0.05, 0.5, 1, 5, 8, and 24 h after dosing with Cy7-Lf_{caps} and Cy7-Lf. Insert shows respective fluorescence in mouse liver.

Very low fluorescence of Cy7-Lf_{caps} in the initial digestion phase (0.05 h) could be attributed to a self-quenching effect due to high local concentration of dye in the intact capsules. Once the capsules reach small intestine they are digested releasing Lf that is diluted in the chymus. As a

result fluorescence signal increases dramatically as proved by *in vivo* full body imaging and *ex vivo* analysis of the mouse GIT (see Figures 6, 7). Released Lf and its digested fragments are adsorbed into the bloodstream .The level of this adsorption may be estimated using the intensity of fluorescence in mouse liver shown in the Figure 7, insert. For mice dosed with Cy7-Lf_{caps}, this intensity increases in the time span from 1 to 5 h post-administration and then remains relatively stable over 24 h. However for mice in the control group dosed with Cy7-Lf the liver fluorescence was always comparable to the autofluorescence level of $(2\text{-}7)\cdot 10^7$ p/s/cm^2/sr. Thus encapsulation in BSA/TA shells ensures 2-4 times higher levels of Lf in the blood stream compared to free Lf. However amount of Lf that reaches caecum/appendix and colon were comparable for both encapsulated and free Lf.

CONCLUSION

In this work for the first time we introduce the LbL assembled (BSA-TA) microcapsules as a system for encapsulation and oral delivery of Lf as bioactive ingredient. Its efficiency is demonstrated using *in vitro* digestion model and *in vivo* small animal model. Absorption by freshly prepared porous $CaCO_3$ microparticles followed by LbL assembly of the BSA-TA shell and dissolution of the cores was suggested as the most efficient and less harmful Lf loading method. One preparation sample of the capsules contains 0.72 mg of native Lf. The Lf distribution among the capsules was normal (or Gaussian) with a span of 0.92 underpinning good capsule loading over population of capsules in the sample. The capsules showed high stability in simulated gastric conditions and effective protection of encapsulated proteins (DQ™ Red BSA) from gastric digestion. Protective efficiency was found to be 76 ± 6% and 85 ± 2%, for $(BSA\text{-}TA)_4$ and $(BSA\text{-}TA)_8$ shells, correspondingly. The shells are degraded in the simulated intestinal

conditions releasing the proteins at their beneficial site of action. *In vivo* experiments confirm that encapsulated Lf is released in the small intestine where it is adsorbed into the bloodstream demonstrating 2-4 times higher levels of Lf compared to free Lf.

We believe that suggested encapsulation system has a great potential for oral delivery of a number of various active food ingredients, including lactoferrin and other bioactive proteins, prebiotics, probiotics, fatty acids, natural inhibitors of glycoside hydrolases, and many other ingredients that require protection from gastric digestion and site specific release in the intestine to achieve their full function. Although, for the case of lactoferrin it could easily happen that simple Lf release in the intestine might not be enough to achieve full biological action and more specific targeting to the receptors of GALT might be required. This may be achieved by additional incorporation of gastro-adhesive proteins into the shells and these experiments are currently in progress in our laboratory. In a near future one can expect a progress in this area and the development of foods that will not only provide people with nutrients but stimulate their immune system, improve health and lifestyle.

Acknowledgements

We thank A*STAR, Singapore and Ministry of Business, Innovation and Employment, New Zealand, SG-NZ Foods for Health Grant for financial support of this work (Project 1414024010). The work was also supported by Ministry of Education and Science of the Russian Federation as part of the State task for National Research Mordovia State University, project № 2952 and grant № 14.Z50.31.0004 to support scientific research projects implemented under the

supervision of leading scientists at Russian institutions and Russian institutions of higher education.

We would like to thank Prof. H. Singh (Riddet Institute, New Zealand), and Dr. Nicole Roy (AgResearch Limited, New Zealand) for their kind advices and help in doing this research.

References

(1) Brock, J. H. Lactoferrin – 50 Years on. *Biochem. Cell Biol.* **2012**, *90*, 245-251.

(2) Yao, X.; Bunt, C.; Cornish, J.; Quek, S.-Y.; Wen, J. Oral Delivery of Lactoferrin: A Review. *Int. J. Pept. Res. Ther.* **2013**, *19*, 125-134.

(3) Onishi, H. Lactoferrin Delivery Systems: Approaches for its More Effective Use. *Expert Opin. Drug Delivery* **2011**, *8*, 1469-1479.

(4) Balcao, V. M.; Costa, C. I.; Matos, C. M.; Moutinho, C. G.; Amorim, M.; Pintado, M. E.; Gomes, A. P.; Vila, M. M.; Teixeira, J. A. Nanoencapsulation of Bovine Lactoferrin for Food and Biopharmaceutical Applications. *Food Hydrocolloids* **2013**, 3*2*, 425-431.

(5) Onishi, H.; Machida, Y.; Koyama, K. Preparation and *In Vitro* Characteristics of Lactoferrin-Loaded Chitosan Microparticles. *Drug Dev. Ind. Pharm.* **2007**, 33, 641-647.

(6) Bengoechea, C.; Peinado, I.; McClements, J. D. Formation of Nanoparticles by Controlled Heat Treatment of Lactoferrin: Factors Affecting Particles Characteristics. *Food Hydrocolloid*s, **2011**, *25*, 1354-1360.

(7) Yao, X.; Bunt, C.; Cornish, J.; Quek, S. Y., Wen, J. Oral Delivery of Bovine Lactoferrin by Using Pectin- and Chitosan-Modified Liposomes and Solid Lipid Particles: Improvement of Stability of Lactoferrin. *Chem. Biol. Drug Des.* **2015**, *86*, 466-475.

(8) Takeuchi, T.; Jyonotsuka, T.; Kamemori, N.; Kawano, G.; Shimizu, H.; Ando, K.; Harada E. Enteric-formulated Lactoferrin Was More Effectively Transported into Blood Circulation from Gastrointestinal Tract in Adult Rats. *Exp. Physiol.* **2006**, *91*, 1033-1040.

(9) Troost, F. J.; Saris, W. H.; Brummer, R. J. Orally Ingested Human Lactoferrin Is Digested and Secreted in the Upper Gastrointestinal Tract *In Vivo* in Women with Ileostomies. *J. Nutr.* **2002**, *132*, 2597-2600.

(10) Yamano, E.; Miyauchi, M.; Furusya, H.; Kawazoe, A.; Ishikado, A.; Makino, T.; Tanne, K.; Tanaka, E.; Takata, T. Inhibitory Effects of Orally Administrated Liposomal Bovine Lactoferrin on the LPS-Induced Osteoclastogenesis. *Lab. Invest.* **2010**, *90*, 1236-1246.

(11) Ishikado, A.; Imanaka, H.; Takeuchi, T.; Harada, E.; Makino, T. Liposomalization of Lactoferrin Enhanced it's Anti-Inflammatory Effects *Via* Oral Administration. *Biol. Pharm. Bull.* **2005**, *28*, 1717-1721.

(12) Ogue, S.; Takahashi, Y.; Onishi, H.; Machida, Y. Preparation of double liposomes and their efficiency as an oral vaccine carrier. *Biol Pharm Bull.* **2006**, *29*, 1223-1228.

(13) Nojima, Y.; Suzuki, Y.; Iguchi, K.; Shiga, T.; Iwata, A.; Fujimoto, T.; Yoshida, K.; Shimizu, H.; Takeuchi, T.; Sato, A. Development of Poly(Ethylene Glycol) Conjugated Lactoferrin for Oral Administration. *Bioconjug. Chem.* **2008**, *19*, 2253–2259.

(14) Bailon, P.; Won, C. Y. PEG-modified Biopharmaceuticals. *Expert Opin. Drug Deliv.* **2009**, *6*, 1-16.

(15) Trif, M.; Guillen, C.; Vaughan, D. M.; Telfer, J. M.; Brewer, J. M.; Roseanu, A.; Brock, J. H. Liposomes as Possible Carriers for Lactoferrin in the Local Treatment of Inflammatory Diseases. *Exp. Biol. Med. (Maywood)* **2001**, *226*, 559-564.

(16) Antipov, A. A.; Sukhorukov, G. B.; Leporatti, S.; Radtchenko, L.; Donath, E.; Mohwald, H. Polyelectrolyte Multilayer Capsule Permeability Control. *Colloids Surf., A* **2002**, *198-200*, 535–541.

(17) Antipov, A. A.; Sukhorukov, G. B.; Donath, E.; Mohwald, H. Sustained Release Properties of Polyelectrolyte Multilayer Capsules. *J. Phys. Chem. B* **2001**, *105*, 2281-2284.

(18) De Geest, B. G.; Sanders, N. N.; Sukhorukov, G. B.; Demeester, J.; De Smedt, S.C. Release Mechanisms for Polyelectrolyte Capsules // Chem. Soc. Rev., 2007, 36, pp. 636−649.

(19) De Cock, L. J.; De Koker, S.; De Geest, B. G.; Grooten, J.; Vervaet, C.; Remon, J. P.; Sukhorukov, G. B.; Antipina, M. N. Polymeric Multilayer Capsules in Drug Delivery. *Angew. Chem., Int. Ed. Engl.* **2010**, *49*, 6954−6973.

(20) Delcea, M., Mohwald, H., Skirtach, A. G. Stimuli-Responsive LbL Capsules and Nanoshells for Drug Delivery. *Adv. Drug Delivery Rev.* **2011**, *63*, 730−747.

(21) Antipina, M. N.; Kiryukhin, M.V.; Skirtach, A.G.; Sukhorukov G.B. Micropackaging *via* Layer-By-Layer Assembly: Microcapsules and Microchamber Arrays. *Int. Mater. Rev.* **2014**, *59*, 224-244.

(22) Shchukin, D. G.; Patel, A. A.; Sukhorukov, G. B.; Lvov, Y. M. Nanoassembly of Biodegradable Microcapsules for DNA Encasing. *J. Am. Chem. Soc.* **2004**, *126*, 3374−3375.

(23) De Geest, B. G.; Vandenbroucke, R. E.; Guenther, A. M.; Sukhorukov, G. B.; Hennink, W. E.; Sanders, N. N.; Demeester, J.; De Smedt, S. C. Intracellularly Degradable Polyelectrolyte Microcapsules. *Adv. Mater.* **2006**, *18*, 1005−1009.

(24) Borodina, T.; Markvicheva, E.; Kunizhev, S.; Mohwald, H.; Sukhorukov, G. B.; Kreft, O. Controlled Release of DNA from Self-Degrading Microcapsules. *Macromol. Rapid Commun.* **2007**, *28*, 1894−1899.

(25) Marchenko, I.; Yashchenok, A.; Borodina, T.; Bukreeva, T.; Konrad, M.; Mohwald, H.; Skirtach, A. Controlled Enzyme-Catalyzed Degradation of Polymeric Capsules Templated on $CaCO_3$: Influence of the Number of LbL Layers, Conditions of Degradation, and Disassembly of Multicompartments. *J. Control. Release* **2012**, *162*, 599−605.

(26) She, Z.; Antipina, M. N.; Li, J.; Sukhorukov, G. B. Mechanism of Protein Release from Polyelectrolyte Multilayer Microcapsules. Biomacromolecules **2010**, *11*, 1241−1247.

(27) De Cock, L. J.; De Wever, O.; Van Vlierberghe, S.; Vanderleyden, E.; Dubruel, P.; De Vos, F.; Vervaet, C.; Remon, J. P.; De Geest, B. G. Engineered $(hep/pARG)_2$ Polyelectrolyte Capsules for Sustained Release of Bioactive TGF-β1. *Soft Matter* **2012**, *8*, 1146−1154.

(28) She, Z.; Wang, C.; Li, J.; Sukhorukov, G. B.; Antipina, M. N. Encapsulation of Basic Fibroblast Growth Factor by Polyelectrolyte Multilayer Microcapsules and Its Controlled Release for Enhancing Cell Proliferation. *Biomacromolecules* **2012**, *13*, 2174−2180.

(29) De Koker, S.; De Geest, B. G.; Singh, S. K.; De Rycke, R.; Naessens, T.; Van Kooyk, Y.; Demeester, J.; De Smedt, S. C.; Grooten, J. Polyelectrolyte Microcapsules as Antigen Delivery Vehicles to Dendritic Cells: Uptake, Processing, and Cross-Presentation of Encapsulated Antigens. *Angew. Chem., Int. Ed. Engl.* **2009**, *48*, 8485−8489.

(30) De Geest, B. G.; Willart, M. A.; Hammad, H.; Lambrecht, B. N.; Pollard, C.; Bogaert, P.; De Filette, M.; Saelens, X.; Vervaet, C.; Remon, J. P.; Grooten, J.; De Koker, S. Polymeric Multilayer Capsule-Mediated Vaccination Induces Protective Immunity Against Cancer and Viral Infection. *ACS Nano* **2012**, *6*, 2136−2149.

(31) De Koker, S.; Naessens, T.; De Geest, B. G.; Bogaert, P.; Demeester, J.; De Smedt, S.; Grooten, J. Biodegradable Polyelectrolyte Microcapsules: Antigen Delivery Tools with Th17 Skewing Activity after Pulmonary Delivery. *J. Immunol.* **2010**, *184*, 203−211.

(32) Sadovoy, A. V.; Lomova, M. V.; Antipina, M. N.; Braun, N. A.; Sukhorukov, G. B.; Kiryukhin, M. V. Layer-by-Layer Assembled Multilayer Shells for Encapsulation and Release of Fragrance. *ACS Appl. Mater. Interfaces* **2013**, *5*, 8948−8954.

(33) Lomova, M. V.; Brichkina, A. I.; Kiryukhin, M. V.; Vasina, E. N.; Pavlov, A. M.; Gorin, D. A.; Sukhorukov, G. B.; Antipina, M. N. Multilayer Capsules of Bovine Serum Albumin and Tannic Acid for Controlled Release by Enzymatic Degradation. *ACS Appl. Mater. Interfaces* **2015**, *7*, 11732-11740.

(34) Lomova, M. V.; Sukhorukov, G. B.; Antipina, M. N. Antioxidant Coating of Micronsize Droplets for Prevention of Lipid Peroxidation in Oil-in-Water Emulsion. *ACS Appl. Mater. Interfaces*, **2010**, *2*, 3669–3676.

(35) Volodkin, D. V.; Larionova, N. I.; Sukhorukov, G. B. Protein Encapsulation via Porous $CaCO_3$ Microparticles Templating. *Biomacromolecules*, **2004**, *5*, 1962−1972.

(36) Minekus, M.; Alminger, M.; Alvito, P.; Ballance, S.; Bohn, T.; Bourlieu, C.; Carriere, F.; Boutrou, R.; Corredig, M.; Dupont, D.; Dufour, C.; Egger, L.; Golding, M.; Karakaya, S.; Kirkhus, B.; Le Feunteun, S.; Lesmes, U.; Macierzanka, A.; Mackie, A.; Marze, S.; McClements, D. J.; Menard, O.; Recio, I.; Santos, C. N.; Singh, R. P.; Vegarud, G. E.; Wickham, M. S.; Weitschies, W.; Brodkorb, A. A Standardised Static *In Vitro* Digestion Method Suitable for Food - an International Consensus. *Food Funct.* **2014**, *5*, 1113-1124.

(37) Bradford, M. M. A Rapid and Sensitive Method for the Quantitation of Microgram Quantities of Protein Utilizing the Principle of Protein-Dye Binding. *Anal. Biochem.* **1976**, *72*, 248-254.

(38) Yakovlev, N. L.; Kiryukhin, M. V.; Antipina, M. N.; Susanto, T. T.; Ravi, S.; Adithyavairavan, M.; Sukhorukov G. B. Secondary Ion Mass Spectrometry of Macromolecules Loading in Individual Polyelectrolyte Multilayer Microcapsules. *Aust. J. Chem.*, **2011**, *64*, 1293-1296.

(39) Stein, W. H.; Moore, S. Amino Acid Composition of Beta-Lactoglobulin and Bovine Serum Albumin. *J. Biol. Chem.* **1949**, *178*, 79−71.

(40) Kunjachan, S.; Gremse, F.; Theek, B.; Koczera, P.; Pola, R.; Pechar, M.; Etrych, T.; Ulbrich, K.; Storm, G.; Kiessling, F.; Lammers, T. Noninvasive Optical Imaging of Nanomedicine Biodistribution. *ACS Nano* **2013**, *7*, 252–262.